CRYRING@ESR
Beam Instrumentation for the RFQ injector linac (Version 0.3)

A. Reiter, W. Kaufmann
Beam Instrumentation LO-BI
2nd April 2013

Abstract

This document proposes a monitoring system for RFQ linac and debuncher cavity of the CRYRING@ESR installation. The system is based on capacitive pickup signals and tank signals, derived by strongly attenuating out-coupling loops in a tank or cavity for the on-line monitoring of the RF power.

At the Manne Siegbahn Laboratory in Sweden, the only the RFQ injector was in operation. In this case, the main operational parameter was the power level of the RFQ amplifier.
For the CRYRING installation at GSI a second RF component, the debuncher, will be added after the RFQ. This device reduces the momentum spread of the particle bunch to be injected into the CRYRING and serves to optimise the injection efficiency. Therefore, the number of operating parameters of the injector linac, consisting now of RFQ and debuncher, is increased to the three parameters RFQ power, debuncher power and debuncher phase with respect to the fixed RFQ phase. This new scheme requires a monitoring system which allows to set up the correct operating point of the debuncher and to monitor its effect on the bunched particle beam.

Table Of Contents

1 INTRODUCTION 4
1.1 Injector Linac for CRYRING 4

2 BEAM INSTRUMENTATION OVIEVIEW 7
2.1 Device Description 7
2.1.1 Capacitive Pickup DB 340 7
2.1.2 Capacitive Pickup DB 490 7
2.1.3 Tank Signal 7
2.2 Monitoring System of Injector Linac 8
2.2.1 Pickup Installation Positions 8
2.2.2 Monitoring Scheme & Measurement Combinations 8
2.2.3 Flight Times as Function of RFQ Energy 9
2.2.4 Bunch Number 9
2.2.5 Estimate of Energy Resolution 10
2.2.6 Energy Shift by Debuncher 10

3 PARMTEQ SIMULATIONS & SIGNAL ESTIMATES 12
3.1 Simulation of RFQ and debuncher 12
3.2 Calculation of Pickup Signals 15
3.2.1 Pickup Signal Estimate 15
3.2.2 Pickup Signals after Drift Space 16

4 DATA ACQUISITION SYSTEM 19
4.1 DAQ Hardware 19
4.1.1 Signal Amplification 19
4.1.2 Signal Acquisition 19
4.1.3 Signal Selection Matrix 20
4.2 DAQ Software 22

5 OVERVIEW OF DEVICES 23

APPENDIX A TECHNICAL DRAWINGS OF DB 340 24

APPENDIX B PICTURES OF RFQ AND DEBUNCHER 25

APPENDIX C MEASURED RFQ ENERGY SPECTRA 29

DOCUMENT HISTORY

Version	Author	Date	Comment
0.1	A. Reiter	March 2013	Document creation
0.2	A. Reiter	02/04/2013	• Correction Table 2 (time shift due to debuncher) • Correction Caption of Fig. 5 (beam spot after 60 cm drift, not RFQ exit!) • Add Table 5 of signal levels in section 4.1.1 for proposed amplifier chain.
0.3	A. Reiter	17/08/2013 23/08/2013	• Changes in beam line after RFQ due to vacuum valve installation. PHP and KVI diagnostics are affected. Feedback from WK for new PHP positions. • Update amplifier description (now: UNILAC type) • Update source information: Plasmatron source, 2 µA maximum current after RFQ for protons

1 Introduction

This document describes the beam instrumentation (BI) for the stand-alone RFQ injector linac of the CRYRING installation in Cave B of the existing GSI facility. The injector consists of a 300 keV/u RFQ (radio-frequency quadrupole) followed by a debuncher which reduces the energy spread ΔE/E.
The injector linac has mainly three operation parameters which influence the micro-structure of the beam: RFQ power, debuncher power and debuncher phase with respect to the fixed RFQ phase.
A basic monitoring system will be described which allows to set up the correct operating point of the debuncher, i. e. its phase with respect to fixed RFQ phase, and to monitor its effect on the bunched particle beam.

1.1 Injector Linac for CRYRING

Multi-turn injection into the CRYRING is planned from a stand-alone RFQ injector which delivers a 300 keV/u ion beam for ion species with charge-to-mass ration q/A > 0.25. The new layout is a modified, more compact injector line compared to the MSL installation.

- DC ion source:
  - Hot discharge source
  - Singly-charged ions or molecules
  - Plasmatron source (Email A. Simonnson to M. Lestinsky, 5th Aug. 2013)
  - 40 kV high voltage platform
  - Beam current: 10-100 µA (typical), $I_{max.}$ = 1 mA (???Check ???)

- Chopper:
  - Installed after ion source and before analysing magnet
  - CAEN High voltage supply & Behlke HV Switch

- RFQ injector:
  - Length 1.54 m
  - RF frequency 108.48 MHz
  - Number of cells 103
  - Electrode voltage 70 kV
  - Ion species q/A > 0.25
  - Input energy 10 keV/u (design value)
  - Output energy 300 keV/u (design value)
  - Beam current: typ. ~10-100 µA
    2 µA maximum for protons with Plasmatron source
  - Pulse length: typ. ~50 µs, max. ~300 µs
  - Repetition rate: < 5 Hz
  - Injection into ring: multi-turn

- Debuncher:
  - Type of cavity: 2-gap spiral resonator
  - Gap length: ???? cm
  - Position: 60 cm after RFQ exit
  - Effective length: ???? cm
  - Maximum effective field: 40 kV

Note that in transport mode ion species with charge-to-mass rations below 0.25 can be transported through the RFQ without acceleration.

Figure 1 shows an overview of the new CRYRING@ESR project in Cave B of the GSI facility. The stand-alone RFQ injector beam line will be shorter compared to the MSL setup in order to fit into Cave B. Figure 2 shows the end part of the RFQ and the following beam line up to the switching dipole YRT1MH2 for the selection of the injection scheme either from the RFQ or the ESR. **Note that the sequence of components has changed!**

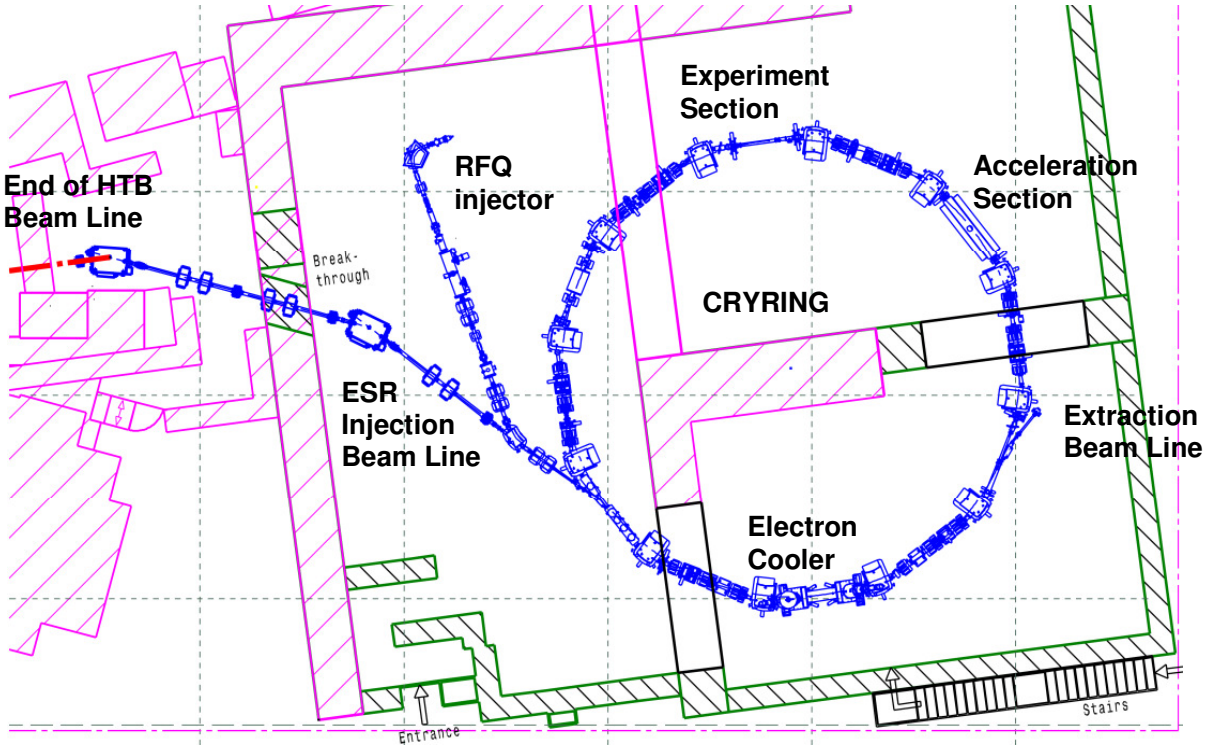

Figure 1: Overview of CRYRING installation in Cave B. The positions of extraction and acceleration section will be changed in the final setup.

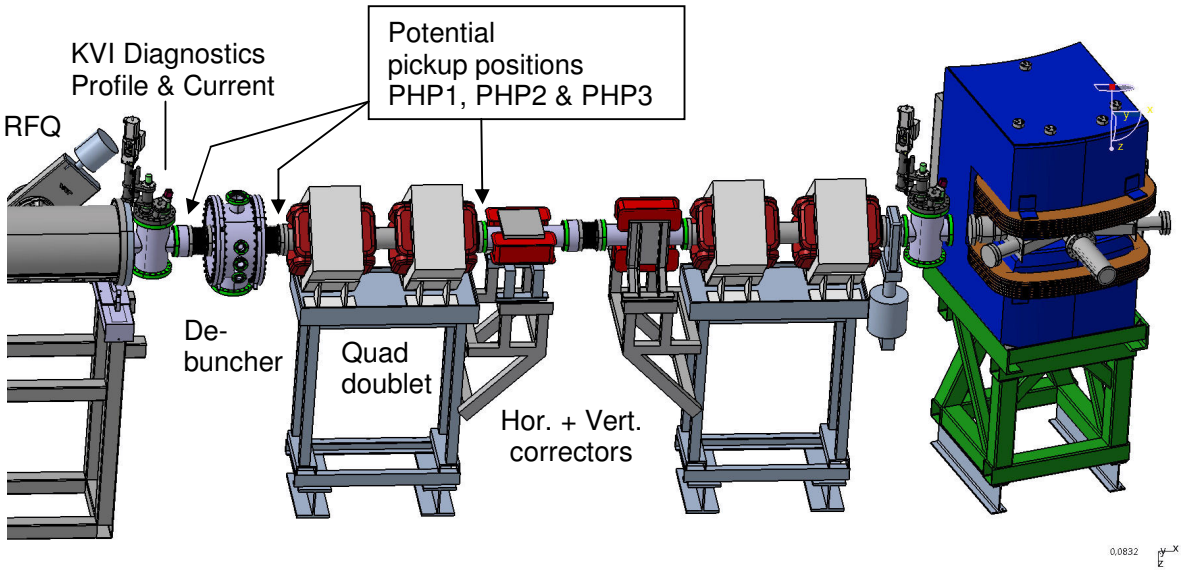

Figure 2: Downstream section of injector line between RFQ exit (left) and switching dipole YRT1MH2. Potential installation positions for pickups are indicated by arrows. The length of the quadrupole section is about 100 cm. Final layout to be defined!

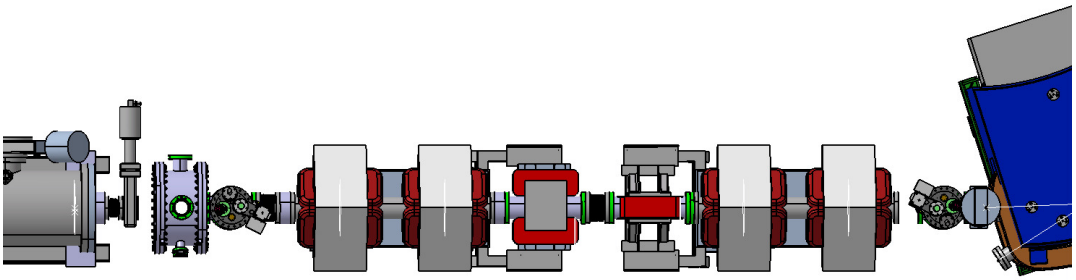

Figure 3: Status 14th August 2013; Proposed layout of components by G. Vorobjev. Following the RFQ (on the left): PHP1 (to be moved to entrance of debuncher), bellows, valve, debuncher, KVI diagnostics, PHP2, quadrupole doublet, PHP3

In August 2013, an update layout of the beam line behind the RFQ was proposed forced by the new vacuum valve installation as shown in Figure 3. This layout will be changed such that PHP1 is installed at the entrance of the debuncher for several reasons:

- The RFQ will emit electrons (see CNAO data for 400 keV/u RFQ of 70 kV electrode voltage, similar to CRYRING RFQ). This current is expected to be in the µA region.
- Sensitive amplifiers of pickups mounted directly on tanks are prone to damage or destruction (as experienced at CNAO and HIT) in case of sparking.
- Since bunches are expected to have a time focus at the debuncher entrance for, a PHP1 position at the debuncher entrance is much more reasonable.

From Figure 2 one may also suspect that viewing screen and Faraday cup measurements with the KVI box mounted at the RFQ exit will be affected by the electron emission from the RFQ.

2 Beam Instrumentation Overview

2.1 Device Description

2.1.1 Capacitive Pickup DB 340

The required installation length of the pickup is 50 mm, the diameter of the protective plate 60 mm. For calculation of the signal shape the following parameters of the inner ring are important:

- Inner radius = 32 mm = 3.2 cm
- Length along beam = 25 mm = 2.5 cm

The pickup DB 340 is of CF100 mounting standard. Technical drawings can be found in the appendix of this document.

2.1.2 Capacitive Pickup DB 490

The required installation length of the pickup is 50 mm, the diameter of the protective plate 50 mm. For calculation of the signal shape the following parameters of the inner ring are important:

- Inner radius = 25 mm = 2.5 cm
- Length along beam = 10 mm = 1.0 cm

The pickup DB 490 has two mounting interface standards CF63 (threaded holes) and CF100 (bore holes).

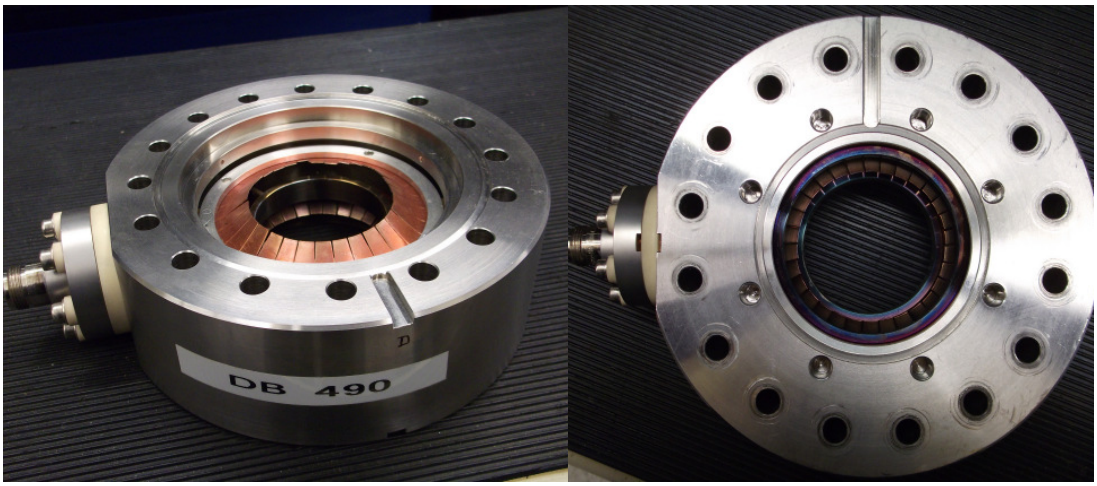

Figure 4: Pictures of a pickup DB 490. The signal is fed to a standard N connector.

2.1.3 Tank Signal

The tank signal is derived from an out-coupling loop which captures a small fraction of the RF power in a tank or cavity. This signal must be appropriately attenuated to fit the voltage range of the data acquisition hardware.

2.2 Monitoring System of Injector Linac

The monitoring system for the injector linac provides data only for accelerated beam, not in transport mode of the RFQ. The minimum beam current required is about 1 µA. The main tasks are setup of the correct relative phase between RFQ and debuncher cavity, and monitoring of the debuncher effect on the beam.

2.2.1 Pickup Installation Positions

Capacitive pickups can be installed only up to a maximum distance behind the RFQ which is mainly given by momentum spread of the particles and RF period. If the drift space L is too long, adjacent bunches start to overlap until, finally, no signal can be detected any more. In the transverse plane, the beam spot size increases along the drift space and for larger distances focussing quadrupoles may become necessary which can influence the TOF measurement.
We assume here that three pickups can be installed in the following sequence:

RFQ – PHP1 – Debuncher – PHP2 – Quadrupole doublet – PHP3

The assumed distance between

- PHP1 and PHP2 is L = 0.5 m, and
- PHP2 and PHP3 is L = 1.0 m.

In this document all calculations are based on the PHP1 and PHP2 combination and a drift space of 0.5 m and a drift space between debuncher and PHP3 of 1.5 m.

2.2.2 Monitoring Scheme & Measurement Combinations

Keeping the RFQ phase as a fixed parameter, and assuming the fore-mentioned installation scheme, the following measurements are required to setup and monitor the injector linac:

No.	Measurement	Signal combination	Comment
M1	RFQ energy (TOF)	PHP1 – PHP2	RFQ energy (debuncher OFF) Energy shift (debuncher ON)
M2	Injection energy (TOF)	PHP2 – PHP3	Monitoring beam energy after debuncher (Quadrupoles ideally OFF; most likely not possible)
M3	Relative TOF (Injection Debuncher)	RFQ – PHP1	Relative RFQ energy (during operation) **OR** use absolute PHP position on scope (trigger synchronised to RF via zero-crossing event)
M4	Phase relation tanks	RFQ – Debuncher	Setup debuncher phase wrt. fixed RFQ phase
M5	Injection Debuncher	PHP1– Debuncher	Monitor RFQ beam stability at debuncher injection (optional)
M6	Phase Debuncher	Debuncher – PHP2	Correct debuncher phase setting No sensitivity on bunch distribution! Short drift -> lower sensitivity, but bunch degradation smaller
M7	Phase Debuncher	Debuncher – PHP3	Correct debuncher phase setting Sensitivity on bunch distribution! Larger drift -> higher sensitivity, but bunch degradation larger

The trigger of the DAQ system – either a digital oscilloscope or a fast sampling ADC module – must be synchronised to the RF master oscillator. This is achieved by a 2-stage logic trigger condition: in the 1st level a TTL high logic defines the macro-pulse timing (gate or arming signal), and in the 2nd level the RF signal zero-crossing defines the trigger timing (trigger event) for the measurement. More information on DAQ requirements can be found in chapter 4.

2.2.3 Flight Times as Function of RFQ Energy

The flight times for particles of different energies around the RFQ design energy of 300 keV/u are given for drift spaces of 0.5 m and 1 m. Two measured energy spectra, one for protons and one for ions, are shown in Appendix C.

Table 1: Particle flight times for 0.5 m and 1 m drift spaces

Energy [keV/u]	Beta	Time-of-flight [ns/0.5 m]	Time-of-flight [ns/m]	Comment
280	0.02451	68.04	136.07	
290	0.02495	66.86	133.71	
300	0.02537	65.73	131.46	Design value Mean proton energy
310	0.02579	64.66	129.32	Mean ion energy
320	0.02621	63.65	127.29	
330	0.02661	62.68	125.35	

The gradient can be estimated to be 0.21 ns/m/(keV/u) = 2.1 ps/cm/(keV/u).

Two small examples are given for illustration:

- For a uniform energy distribution of width ±2% (6 keV/u) around 300 keV/u kinectic energy and a 2 m drift space, the total width Δt of the distribution is Δt = (2 x 0.21 x 2 x 6) ns = 5 ns.

- For the proposed drift space of 0.6 m between RFQ and debuncher (see section 3.1) and a 10 keV/u energy offset from the design value, the arrival time difference at the debuncher is about 1.3 ns or 14 % of the RF period. See also section 2.2.6.

2.2.4 Bunch Number

For the design energy of 300 keV/u, one calculates the following values of basic quantities

- Velocity beta = v/c = 0.0254,
- v~0.76 cm/ns~7 cm/RF period, and
- bunch number N = 7 for a 0.5 m drift space between the pickups.

For the chosen drift spaces, the bunch number changes at the energy of 312 keV/u from 7 to 6, which can be seen as a jump of the measured time-of-flight value in Figure 5.

For the design energy, a bunch number of 8 results in a TOF energy of 230 keV/u and a bunch number of 6 in a TOF energy of 405 keV/u. Therefore, a third pickup is not absolutely necessary to achieve unambiguous results.

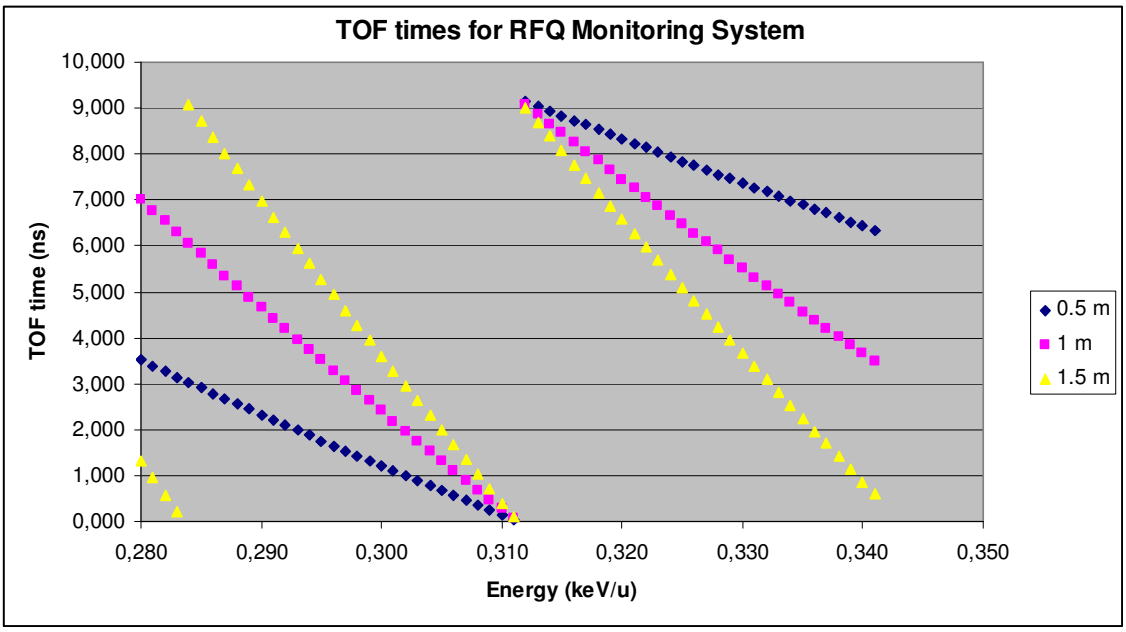

Figure 5: Theoretical TOF (time-of-flight) value on oscilloscope for energies between 290 and 330 keV/u. The drift space is assumed to be 0.5, 1.0 or 1.5 meter.

2.2.5 Estimate of Energy Resolution

If it is possible to install two identical pickups in the straight section after the RFQ and before the quadrupole doublet, energy measurements by time-of-flight can be carried out while the debuncher is switched off. In this case, we assume a drift length of 500 mm. During operation the second pickup may be used to optimise the debuncher phase, but not the debuncher power level (no change in bunch structure and hence pickup signal due to short drift). This can only be achieved with a pickup installed at a reasonable distance to the debuncher, in the present case PHP3.

Then, one can derive

- an uncertainty ΔE_{TOF} = 0.44 keV/u (~0.15 %) for a timing uncertainty Δt = 50 ps, and
- an uncertainty ΔE_{MEC} = 0.58 keV/u for an uncertainty in the pickup distance ΔL = 0.5 mm due to mechanical tolerances.

The former uncertainty defines the TOF measurement resolution as the mechanical error is fixed.

The achievable timing uncertainty Δt will depend on various experiment parameters, but 50 ps is regarded as a safe upper limit from previous measurements with 400 keV/u RFQs of the therapy facilities HIT and CNAO. There, the energy resolution was about 10 ps.

Note that the beam spot sizes in PHP1 and PHP2 differ significantly. At the latter position the beam spot may be as large as 4 cm (see Figure 6 of section 3.1). The DB 490 pickup diameter is 5 cm.

2.2.6 Energy Shift by Debuncher

The energy shift ΔE of a particle of charge q and atomic mass A when passing through an effective voltage V_{eff} is calculated as:

$$\Delta E\,[\mathrm{keV/u}] = (q/A) \cdot V_{\mathrm{eff}}\,[\mathrm{kV}]$$

The effective voltage V_{eff} of the debuncher is assumed to be 40 kV. Therefore, the maximum energy shift at this nominal voltage is

$$\Delta E\,[\mathrm{keV/u}] = (q/A) \cdot V_{\mathrm{eff}}\,[\mathrm{kV}] = 40 \cdot (q/A)\,[\mathrm{kV}]$$

Table 2 contains the maximum energy shift ΔE of some previously used ions and molecules at MSL for an assumed effective voltage of 40 kV. The flight time difference Δt to a pickup at 10 cm distance for particles with energy offset ΔE with respect to the 300 keV/u design energy is given in the last two rows. The time differences can be approximated using the gradient of 0.21 ns/m/(keV/u) of section 2.2.3.

Even for this rather short drift space, the time offset Δt should be detectable for heavier particles with masses around A~50 (ΔE~1 keV/u). A higher debuncher field would be beneficial for the setup of the correct zero-phase. If a third pickup PHP3 can be mounted after the quadrupole doublet, the time shift would be a factor of 10 larger at the expense of reduced signal amplitude due to overlap of adjacent bunches (see subsection 3.2.2).

Practically, the difference Δt is measured by comparing the relative timing between debuncher tank signal and pickup signal PHP2 or PHP3 on a GSa/s digital oscilloscope.

Table 2: Energy shift for nominal debuncher value of 40 kV and time offset for 10 cm drift space. Some previously stored singly-charged ions or molecules were selected from available publications.

Ion species	Charge q	Atomic mass A	ΔE [keV/u]	Time offset Δt [ns]	[ps]
Proton	1	1	+40	-0.748	-750
H_3^+	1	3	+13	-0.264	-265
H_2^+	1	2	+20	-0.398	-400
D^+	1	2	+20	-0.398	-400
$^3He^+$	1	3	+13	-0.264	-265
$^4He^+$	1	4	+10	-0.205	-205
$^{14}N^+$	1	14	+2.9	-0.061	-60
$(NH_4)^+$	1	18	+2.2	-0.046	-45
$(N_2D_7)^+$	1	42	+0.95	-0.020	-20
$(N_3D_{10})^+$	1	62	+0.65	-0.014	-14

3 Parmteq Simulations & Signal Estimates

3.1 Simulation of RFQ and debuncher

This section summarises results of Parmteq simulations performed by A. Bechthold (NTG). The information was sent to F. Herfuth on February 7th and is based on input data at the RFQ entrance provided by Gleb Vorobjev or ideal design distributions. The debuncher was simulated using the following assumptions:

- Single gap of 0.5 cm
- Effective voltage 40 kV (R_p= 1 MOhm, 2 kW power level)

Note that the real parameters are not known. These data are to be confirmed!
The pictures in Appendix B show a spiral resonator with two gaps.

The main results were:

- The provided input beam parameters not perfectly matched to RFQ which causes some losses in debuncher due to large divergence in Y coordinate.
- **Proposed drift length between RFQ exit and debuncher is 60 cm.**
- **Energy spread for 95% of particles after RFQ: ±3.5%**
- **Energy spread for 95% of particles after debuncher: ±2 %**

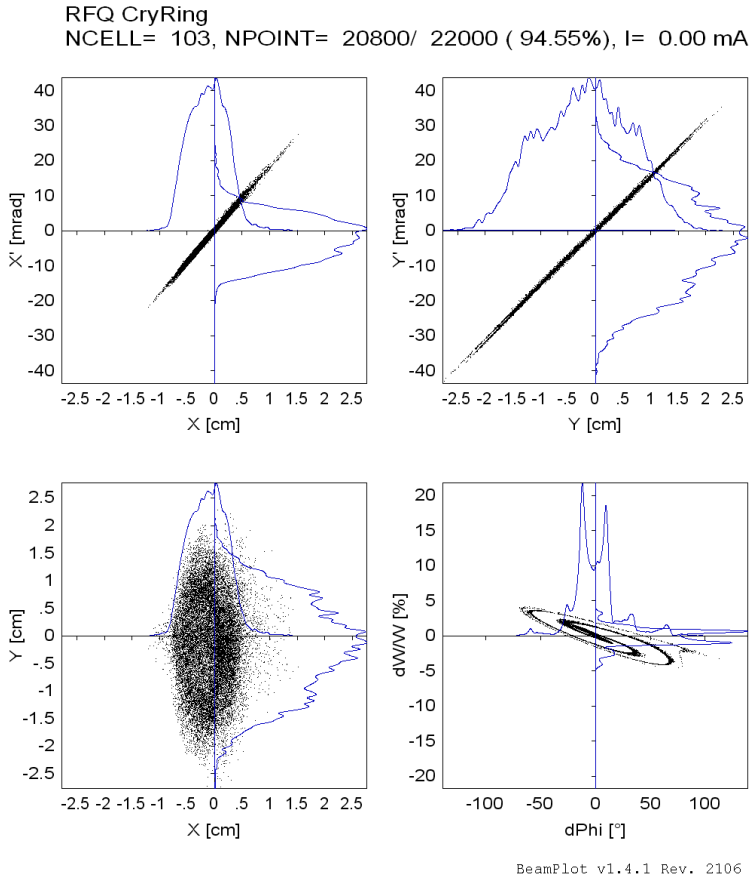

Figure 6: Distributions at distance of 60 cm from RFQ exit for provided input data. ΔE/E= ±3.5% for 95% of particles.

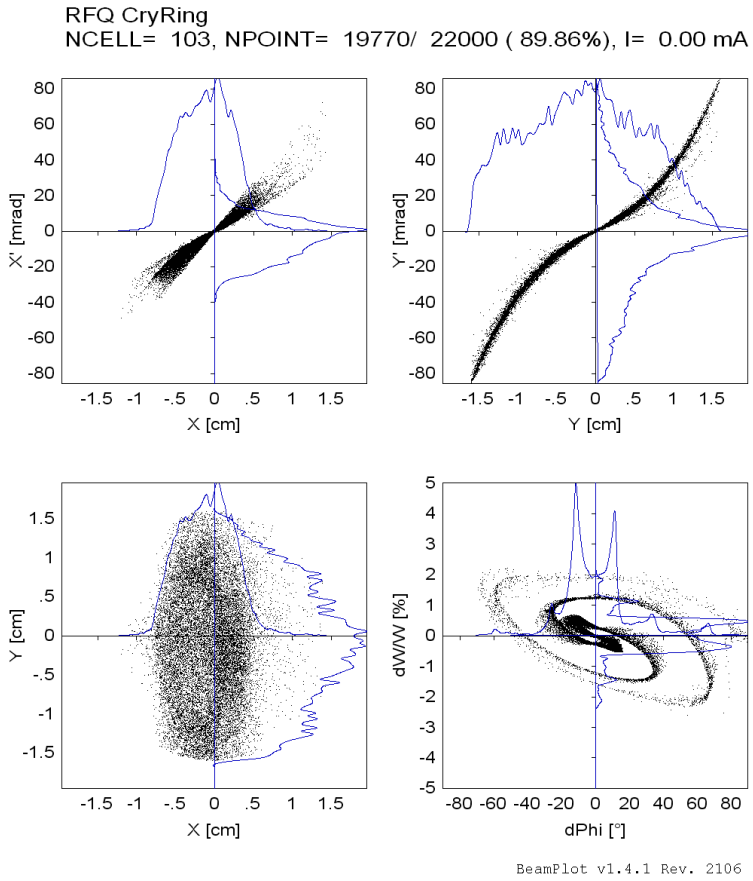

Figure 7: Distributions 7 cm behind debuncher for provided input data. ΔE/E= ±1.8% for 95% of particles.

Open Questions:

Raw data: RFQ exit distribution data at exit (-> Bechthold)
Raw data: Debuncher distribution data at exit and after 1.5 m of drift (Bechthold)

2% energy spread small enough (-> CRYRING ion optics)
Debuncher parameters (-> RF group, Sweden, CRYRING collaboration)

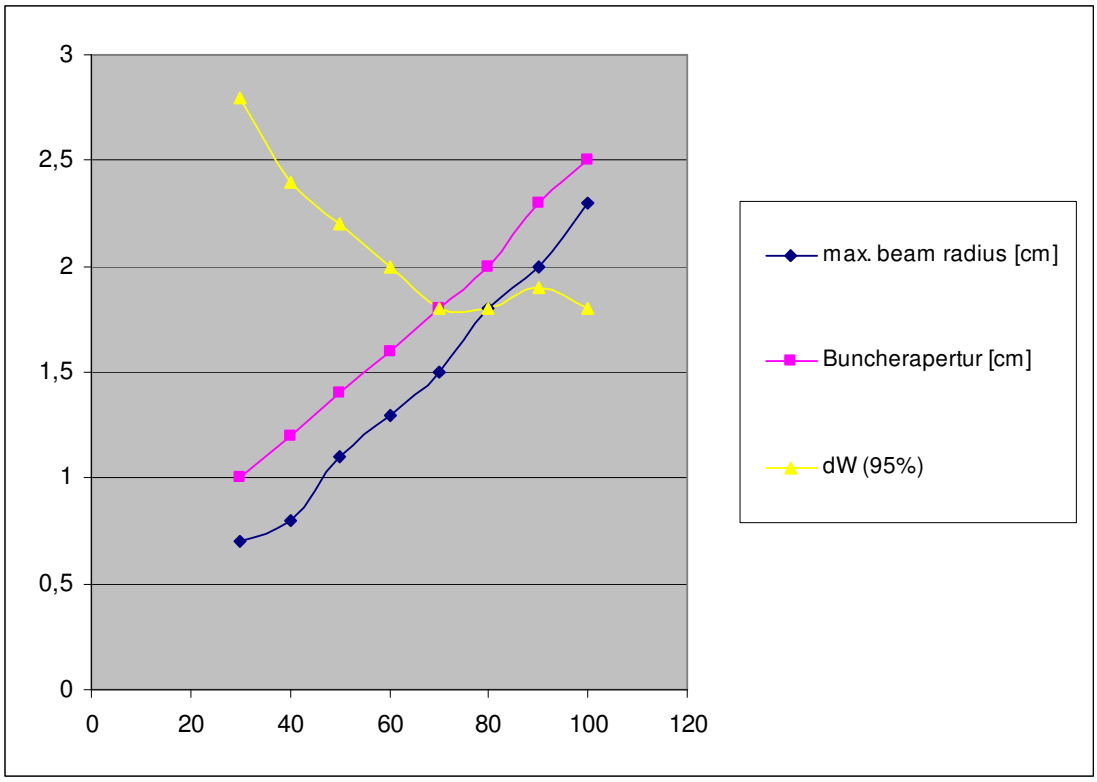

Figure 8: Plot of energy width (%) as function of drift length to debuncher (yellow). The effective voltage was assumed to be 40 kV.

Table 3: Energy width (%) for 95% of particles as function of drift length to debuncher

Drift [cm]	Max. beam radius [cm]	Buncher aperture [cm]	V(buncher) [kV]	dW/W (95%)
30	0,7	1	40	2,8
40	0,8	1,2	40	2,4
50	1,1	1,4	40	2,2
60	1,3	1,6	40	2
70	1,5	1,8	40	1,8
80	1,8	2	40	1,8
90	2	2,3	40	1,9
100	2,3	2,5	40	1,8

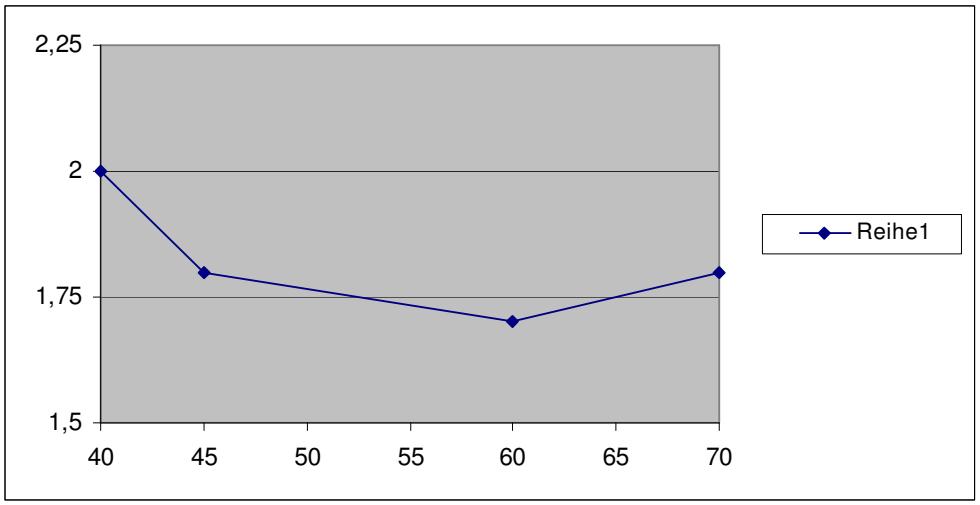

Figure 9: Energy spread (%) after debuncher as function of effective debuncher voltage (kV). Above 40 kV, the assumed voltage for the simulations, the function shows a broad minimum around 50–70 kV.

3.2 Calculation of Pickup Signals

Based on a simple analytical formula for an on-axis particle, the signal shape of a given pickup geometry can easily be calculated. Smearing this single-particle response with the expected bunch distributions, we can estimate the displacement current induced in the pickup ring.
In a second step, one can approximate the pickup response by using the calculated displacement current as input to an RC circuit, the most simple equivalent circuit of a pickup. Typically, the pickup capacitance C is around 10-20 pF and the resistance R is 50 Ohm.

3.2.1 Pickup Signal Estimate

In this section the pulse shape of the capacitive pickup is calculated from a simple model for a single particle. The two main parameters for the signal calculation are the radius R and length L of the pickup ring.

Pickup	Geometry (L x R)	Sensitivity (µV/µA)	Comment
DB 340	2.5 cm x 3.2 cm	~22	Estimated sensitivity 1.4 MeV/u beam energy (GSI) 108 MHz RF frequency
	2.5 cm x 3.2 cm	~15	Calculated sensitivity (simple model) 300 keV/u beam energy
DB 490	1.0 cm x 2.5 cm	~20	Calculated sensitivity (simple model) 300 keV/u beam energy

All calculations in this section were carried out for a pickup of type DB 340. Due to its larger diameter R and length L, the DB 340 signal is broader and of slightly lower amplitude compared to the DB 490, and thus, the calculations represent the worse case.
Figure 10 shows the single-particle response of the pickup, calculated from an analytical formula (blue). The responses of RC circuits with C=10 and 20 pF yield a significantly smaller signal amplitude (green, red). Smearing the response with a Gaussian function with a

standard deviation of 10% of the RF period (~1 ns in the present case) or a uniform distribution of the same total width has little effect on the calculated signal shape (light blue, purple). The latter cases approximate the typical width of a bunch at the exit of an accelerator.

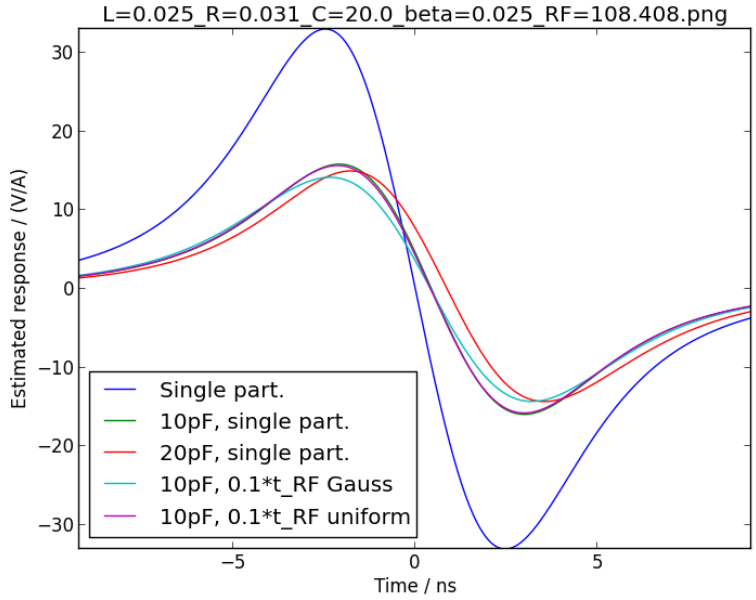

Figure 10: Calculated absolute signal levels for different pickup parameters. The width of the pickup signal exceeds the RF period of 9.2 ns and adjacent signal will overlap. The resistance R is 50 Ohm.

3.2.2 Pickup Signals after Drift Space

In this section the calculation of the pickup signal shape is extended

- by taking into account the arrival time distribution of particles in a bunch and
- by taking into account the overlap between adjacent signals in a periodic bunch train.

In order to estimate the feasibility of monitoring the debuncher effect on the bunch distribution, we have to calculate the signal response of PHP3. Therefore, we limit the discussion on the long drift of 2.0 m length.
Based on the measurements presented in Appendix C, we assume a triangular energy distribution at the start of a drift section in a 5% range around the mean value of 300 keV/u. In Figure 11 the arrival time is shown for a 2.0 m drift. Its total width of 12 ns exceeds the RF period of 9.2 ns which means that adjacent bunches are starting to overlap.

Similar to the case of the 400 keV/u therapy RFQs that operate at twice the frequency of 216.8 MHz, the observable signal shape resembles a sine wave when the overlap is calculated. At the same time the pickup sensitivity is reduced by almost a factor of 6 for a 2.0 meter long drift space, as shown in Figure 12. Therefore, the **signal shape** carries very little to no information at all, merely the **signal amplitude** is an indicator of the bunch width.

The data of Table 3 and the corresponding Figure 13 indicate that between 3.5% (RFQ energy spread) and 2% (after debuncher) the signal level decreases by 50%. Of course, this calculation of a 2.0 m long drift is only a rough approximation of the 2-stage process (RFQ: ΔE/E=3.5% & 0.6 drift to debucher, followed by debuncher ΔE/E=2.0% & 1.5 m drift to PHP). Ideally, a Parmteq simulation should provide the final information.

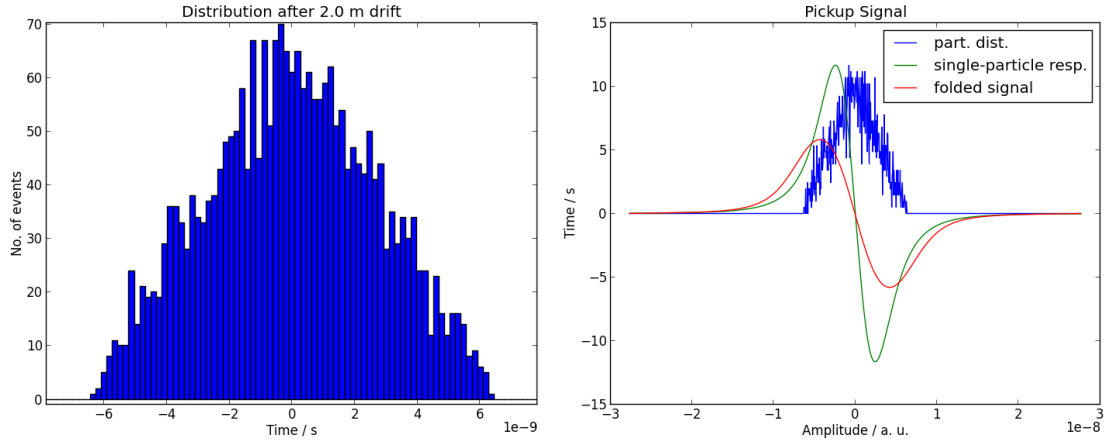

Figure 11: Arrival time distribution after 2.0 m drift (left) and corresponding signal shapes (right) for a total energy width of (300 keV/u ± 5%).

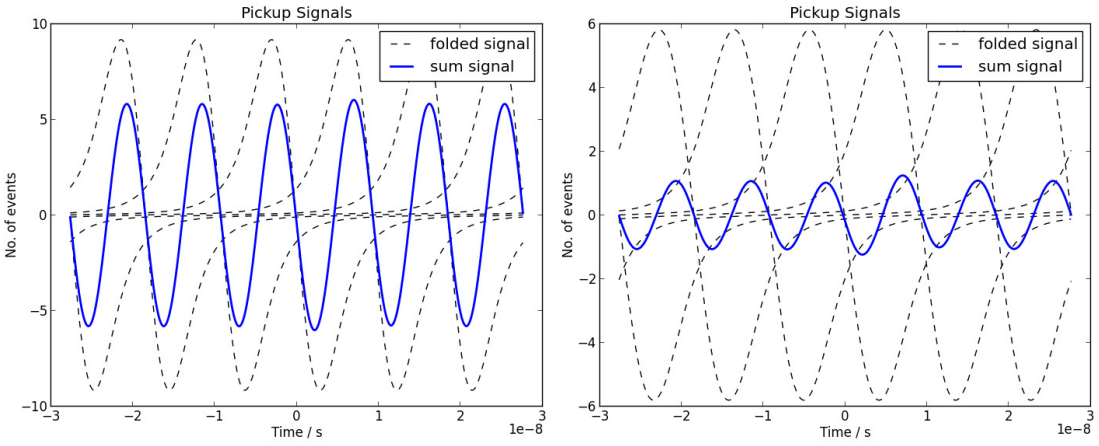

Figure 12: Overlap of adjacent pickup signals for a drift space of 1 m (left) and 2 m (right) and triangular distribution in the range (285–315) keV/u or (300 keV/u ± 5%).

Table 4: Dependence of bunch width and signal level on energy spread for 2.0 m drift

Energy width [%]	Energy range [keV/u]	Width time dist. [ns] after 2.0 m	Signal voltage V_{pp} [rel. units]	Comment
2.0	294-306	5	14	Estimate after debuncher
3.5	290-310	9	7.5	RFQ exit
5.0	285-315	12	2	
7.0	280-320	18	0.5	

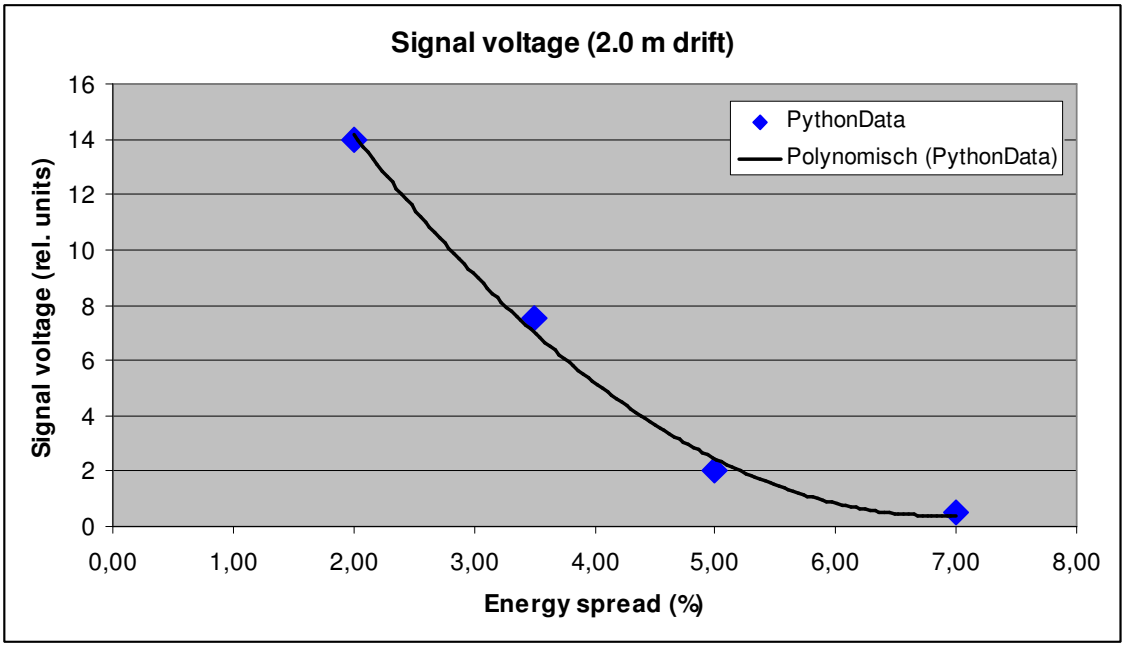

Figure 13: Peak-to-peak voltage as function of energy spread for data of Table 3. Between 2% and 4% a reasonable sensitivity can be expected.

4 Data Acquisition System

4.1 DAQ Hardware

4.1.1 Signal Amplification

The following signal estimates disregard overlap effects that can reduce the signal level considerably (factor of 5).

The rather weak pickup signals must be amplified at the detector stage to preserve the signal-to-noise ratio. Assuming 15 µV/µA sensitivity and a beam current of 1 µA, a 60 dB amplifier produces a signal of 15 mV amplitude or 30 mV_{pp} peak-to-peak voltage. A typical oscilloscope with input range ±5 Volt in 50 Ohm can cope with a maximum beam current of ~350 µA.

Amplifier parameters:

- Amplification -36,….+50 dB, 6 dB steps
- Bandwidth: ???? MHz
- Impedance: 50 Ohm
- Maximum output voltage = ????? Volt V_{pp} (peak-to-peak voltage)
- GSI-type amplifier as for UNILAC. Remote control via ???????????

Table 5 contains expected signal level as function of beam current and two arbitrarily chosen amplifier settings of 30 dB and 60 dB. Note that the maximum value for the UNILAC amplifiers is 50 dB.

Table 5: Pickup signal levels for a two-stage +30/+60 dB amplification chain

Sensitivity (µV/µA)	Mean current (µA)	Mean voltage Vpp (µV)	Voltage amplifier (dB)	Output voltage Vpp (mV)	Switchable amplifier (dB)	Switchable amp. output Vpp (mV)
15			fixed-gain		0 / 30 dB	
	1	30,0	30	0,95	30	30,0
	5	150,0	30	4,74	30	150,0
	10	300,0	30	9,49	30	300,0
	20	600,0	30	18,97	30	600,0
	50	1500,0	30	47,43	30	1500,0
	100	3000,0	30	94,87	0	94,9
	250	7500,0	30	237,17	0	237,2
	500	15000,0	30	474,34	0	474,3

4.1.2 Signal Acquisition

The most straightforward readout system is a digital oscilloscope. If three capacitive pickups are installed, signals from five detectors or tanks must be monitored by the DAQ system. To accommodate these on a single oscilloscope, an RF switching matrix is necessary.

DAQ hardware: 4-channel digital oscilloscope
- Band width: 1 GHz
- Sampling speed: 5 GSa/s (per channel!)
- ADC bits: 10/12 (LeCroy scope) ??? 8 bit ok for standard

monitoring measurements!

Trigger event: logic AND of external gate pulse & zero-crossing of Master Oscillator

DAQ trigger: 2 stage trigger: gate & zero-crossing RF signal (master)
After N-th trigger event (e. g. zero-crossing of RF signal with positive/ negative slope)
(NOTE: Not all digital scopes support this feature!)

The trigger of the DAQ system – either a digital oscilloscope or a fast sampling ADC module – must be synchronised to the RF master oscillator. Copies of the master oscillator signal define the reference clock for the timing of RFQ and debuncher amplifiers.
The synchronisation of the measurement to the RF master is achieved by a 2-stage logic trigger condition, see Figure 14. In the 1st trigger level, a TTL high logic defines the macro-pulse timing (gate or arming signal) and, in the 2nd level, the N-th RF signal zero-crossing of selected slope defines the trigger timing (trigger event) for the measurement. Hereby N is a user-defined integer and the slope may be positive or negative.

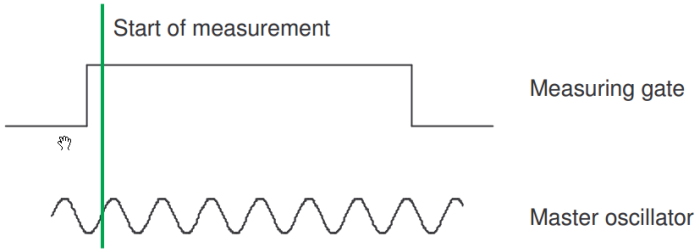

Figure 14: Trigger logic for TOF measurements. Here event number N=1, the trigger is executed at the first occurrence of a zero-crossing event of positive slope.

4.1.3 Signal Selection Matrix

The signal matrix of Table 6 is suggested for a four channel DAQ system. The signals of RFQ and PHP3 are used for relative timing measurements and can hence be connected through an RF switch. The RF switch may be a simple RF relay controlled by an external TTL level or an Ethernet controlled Keithley Integra Series System with RF multiplexer cards. The measurement matrices with RFQ or PHP3 signal are listed in Table 7/Table 8. The measurement numbers refer to those defined in subsection 2.2.2.

Table 6: Signal connection matrix for a 4-channel DAQ system

Channel	Signal	Comment
1	RFQ / PHP3	Relative measurements
2	Debuncher	Relative measurements
3	PHP1	TOF measurement Calibrated cable
4	PHP2	TOF measurement Calibrated cable

Table 7: Possible simultaneous measurements, if RFQ signal is selected

Ch.		1	2	3	4
	Signal	RFQ	Deb.	PHP1	PHP2

1	**RFQ**	x	**M4**	**M3**	x
2	**Deb.**	x	x	**M5**	**M6**
3	**PHP1**	x	x	x	**M1**
4	**PHP2**	x	x	x	x

Table 8: Possible simultaneous measurements, if PHP3 signal is selected

Ch.		**1**	**2**	**3**	**4**
	Signal	**PHP3**	**Deb.**	**PHP1**	**PHP2**
1	**PHP3**	x	**M7**	x	M2
2	**Deb.**	x	x	M5	M6
3	**PHP1**	x	x	x	M1
4	**PHP2**	x	x	X	x

The main purpose of PHP3 signal is the monitoring of the debuncher effect, i. e. the observation of PHP3 signal amplitude as function of debuncher power. This measurement is carried out at the end of the Linac setup procedure. The default selection is therefore the RFQ signal.

4.1.4 Schematic of Electronics

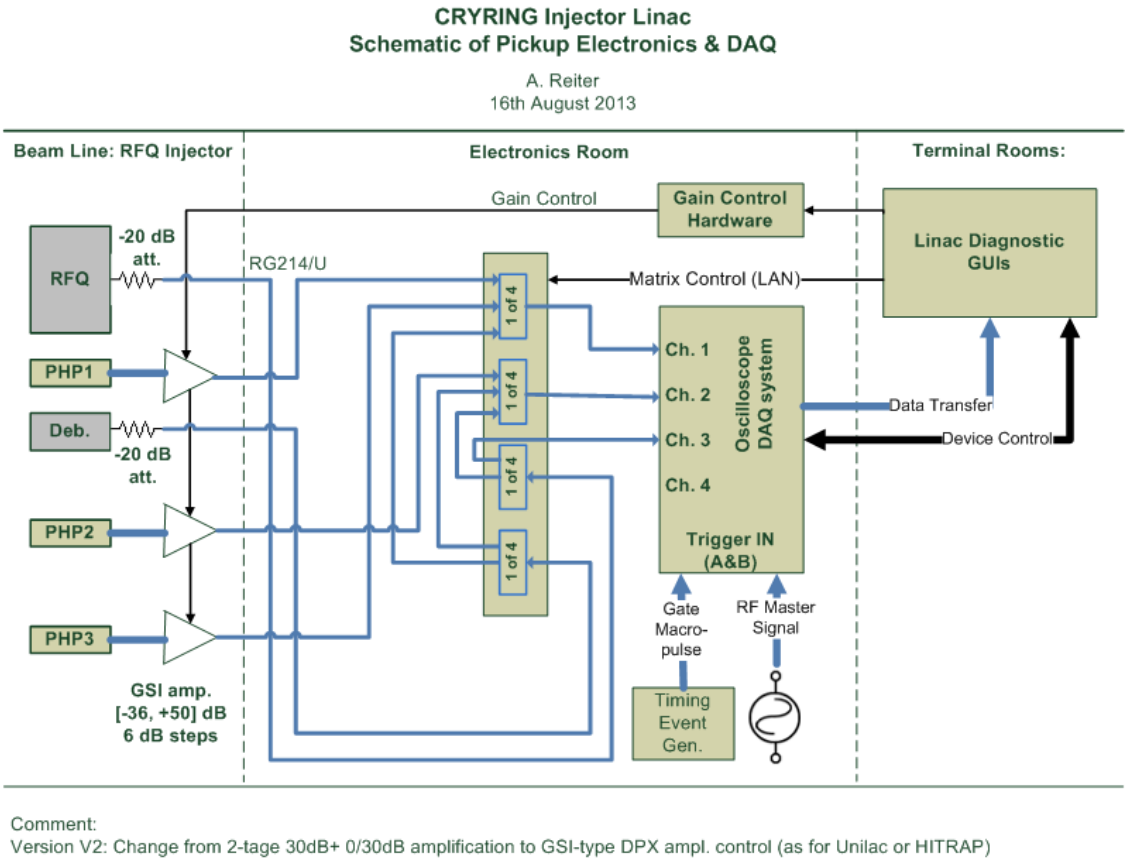

Figure 15: Overview of electronics chain for pickup and tank signals. Final layout to be defined!

4.2 DAQ Software

- Standard data analysis as for HIT, CNAO and HITRAP based on interleaving.

- Observation of beam energy as function of RFQ tank signal voltage V_{pp}. This could be a 2D plot or a simple trending. If beam energy depends on power level, then the power regulation of the RF amplifier (0.1% typically) may be monitored on-line via correlation of beam energy and V_{pp}. Here, we need an oscilloscope of at least 10 bit, better 12 bit, resolution.
  Other option: Demodulation/DC conversion of tank signal & DC measurement

Describe SW. Re-use Python SW of HITRAP? Readout via FESA & Java based on oscilloscope project of Timo?
What are the requirements?
There is no FESA readout of oscilliscopes yet (SOS, soft oscilloscope project of Cosylab)

5 Overview of Devices

CHECK NAMES OF DEVICES

Modified RFQ Injection Line (Source to junction dipole YRT1MH2 with ESR injection line)						
GSI Name	**MSL Name**	**Type**	**Position/ Section**	**Drive**	**HV**	**Comment**
YRT1BR1T		RFQ	L1	No	No	RFQ accelerator
YRT1DP1		PHP1	L1	No	No	Pickup 1
YRT1BB1		Deb.	L1	No	No	debuncher for injection optimisation
YRT1DP2		PHP2	L1	No	No	Pickup 2
YRT1DP3		PHP3	L1	No	No	Pickup 3

Appendix A Technical Drawings of DB 340

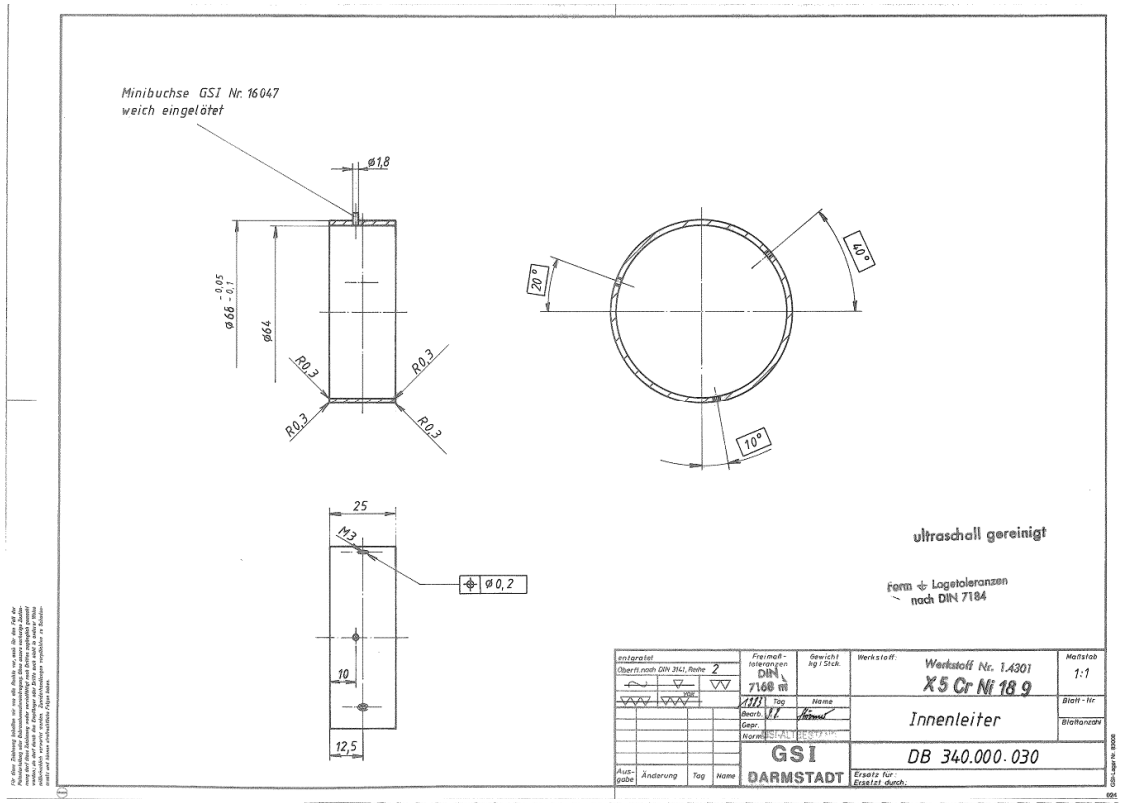

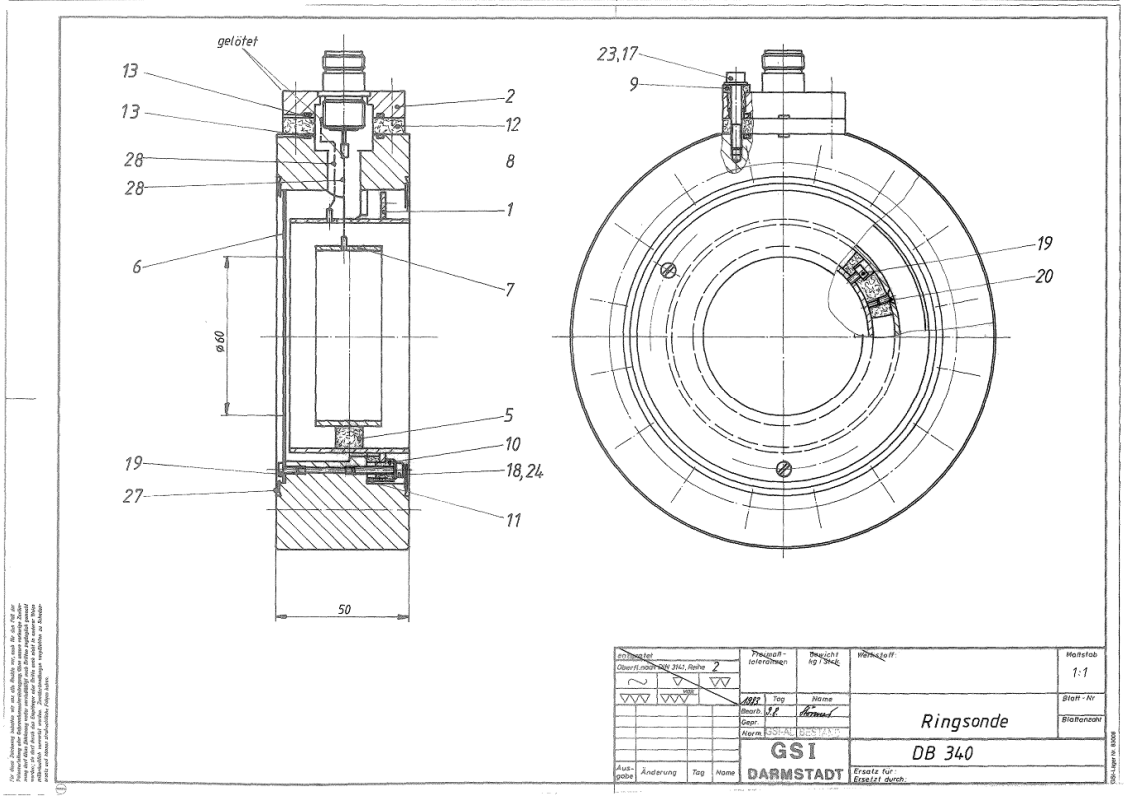

Appendix B Pictures of RFQ and Debuncher

Figure 16: RFQ with connections to out-coupling loops for RF control and reference tank signal for diagnostics. Beam direction right to left.

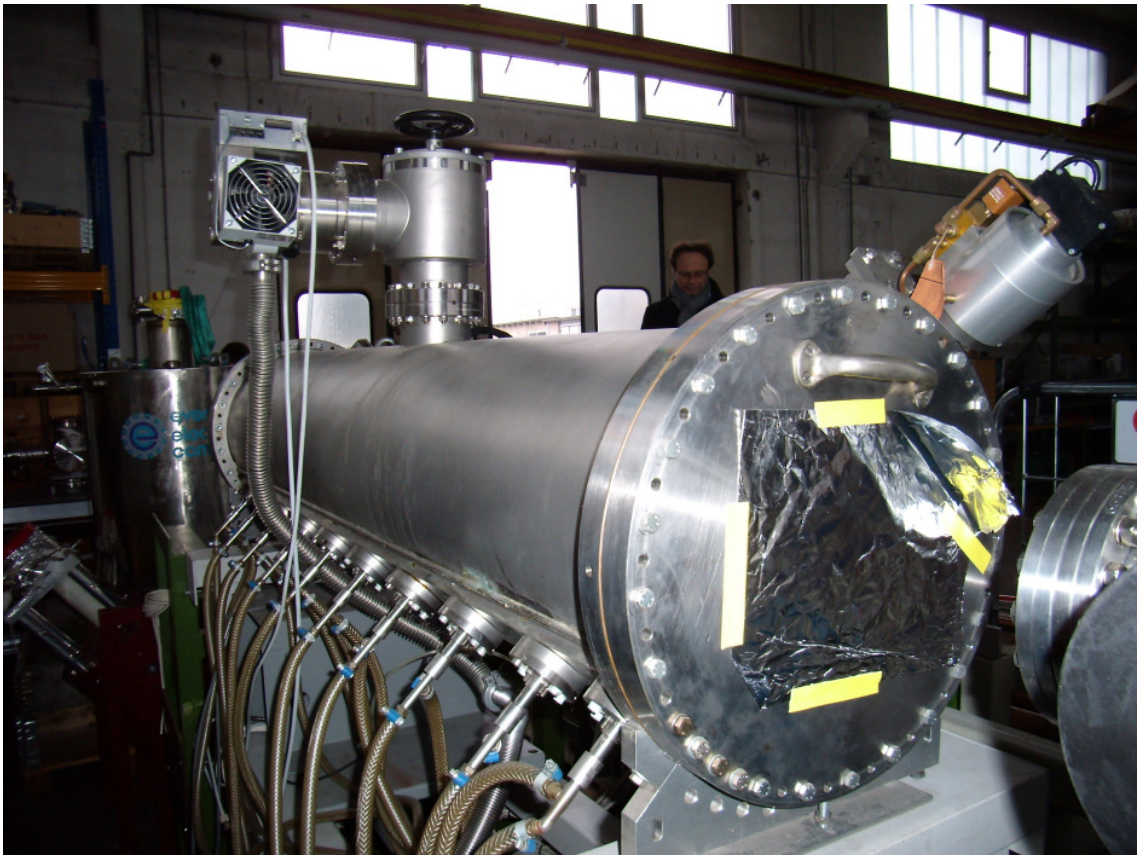

Figure 17: Cooling connections to RFQ stems. Beam direction back to front.

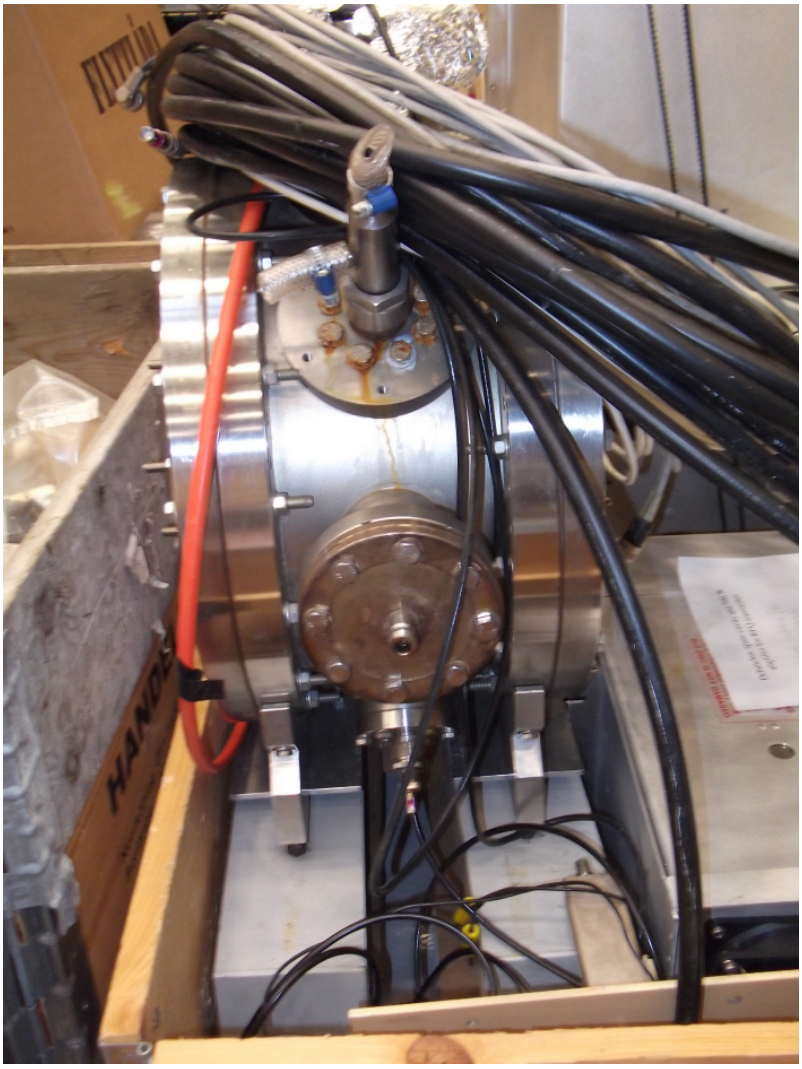

Figure 18: Debuncher, stored in Testing Hall after delivery to GSI.

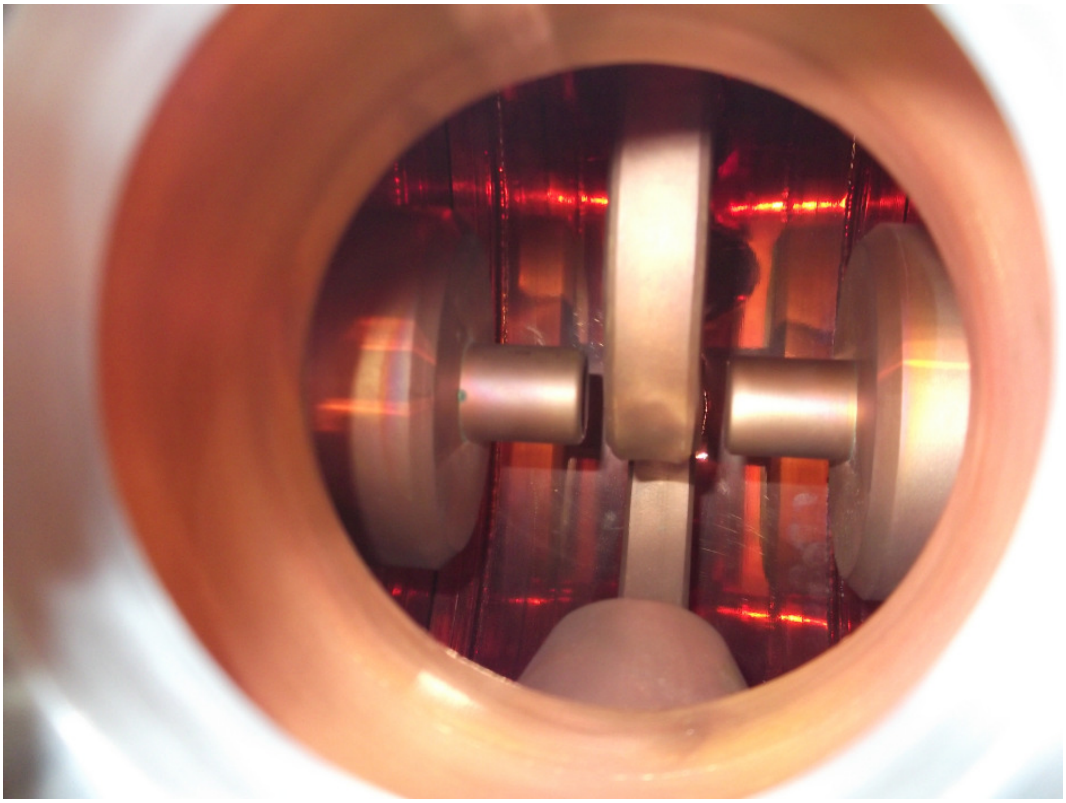

Figure 19: Debuncher, view into cavity through top flange. The two gap geometry of the spiral resonator can be seen.

Appendix C Measured RFQ Energy Spectra

The following two measured RFQ energy spectra were taken from A. Schempp et al.,"'The CRYRING RFQ for Heavy Ion Acceleration", EPAC, 1990, pp. 1231-1233.

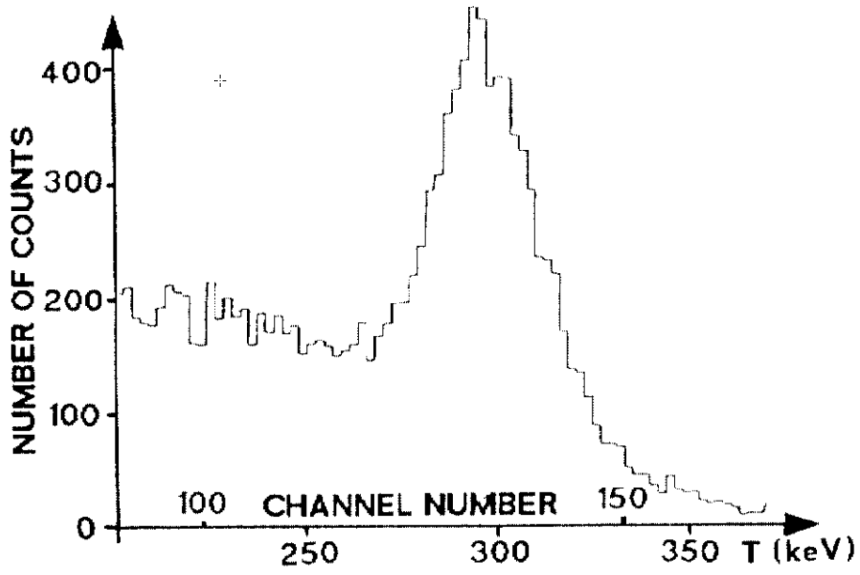

Fig. 9 Energy spectrum for protons

Figure 20: Proton energy spectrum measured with a Si detector after scattering off an Au foil. The total peak width is about ±10%, disregarding the background distribution.

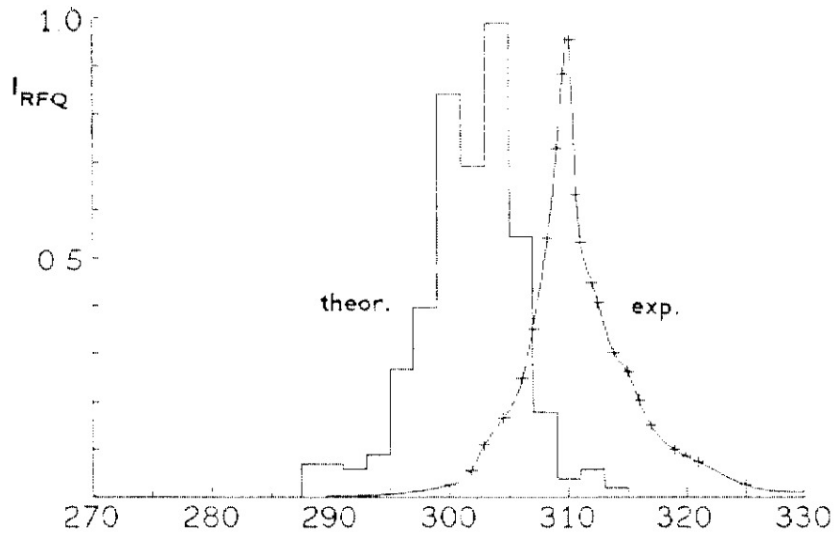

Fig. 4 Ion energy spectra

Figure 21: Measured ion energy spectrum and theoretical prediction. Energy measurement determined with bending magnet and slit system. The total peak width is about ±4%.